ADIMEW: FRACTURE ASSESSMENT AND TESTING OF AN AGED DISSIMILAR METAL WELD PIPE ASSEMBLY

John B Wintle[1], Bridget Hayes[2] and Martin R Goldthorpe[3]
TWI Ltd, Granta Park, Gt Abington, Cambridge CB1 6AL, UK

30th MPA Seminar in conjunction with the 9th German and Japanese Seminar
Stuttgart, October 6 and 7, 2004

ABSTRACT

ADIMEW (Assessment of Aged Piping Dissimilar Metal Weld Integrity) was a three-year collaborative research programme carried out under the EC 5th Framework Programme. The objective of the study was to advance the understanding of the behaviour and safety assessment of defects in dissimilar metal welds between pipes representative of those found in nuclear power plant.

ADIMEW studied and compared different methods for predicting the behaviour of defects located near the fusion boundaries of dissimilar metal welds typically used to join sections of austenitic and ferritic piping operating at high temperature. Assessment of such defects is complicated by issues that include: severe mis-match of yield strength of the constituent parent and weld metals, strong gradients of material properties, the presence of welding residual stresses and mixed mode loading of the defect. The study includes the measurement of material properties and residual stresses, predictive engineering analysis and validation by means of a large-scale test.

The particular component studied was a 453mm diameter pipe that joins a section of type A508 Class 3 ferritic pipe to a section of type 316L austenitic pipe by means of a type 308 austenitic weld with type 308/309L buttering laid on the ferritic pipe. A circumferential, surface-breaking defect was cut using electro discharge machining into the 308L/309L weld buttering layer parallel to the fusion line. The test pipe was subjected to four-point bending to promote ductile tearing of the defect.

This paper presents the results of TWI contributions to ADIMEW including: fracture toughness testing, residual stress measurements and assessments of the ADIMEW test using elastic-plastic, cracked body, finite element analysis.

INTRODUCTION

Dissimilar metal welds (DMWs) are used in pressurised water reactors to connect low alloy, ferritic steel components to the austenitic stainless steel primary pipework. Particular concerns about the fracture behaviour of DMWs arise from the presence of external surface cracks in the ferritic to austenitic interface. Assessment of such defects is complicated by issues such as: severe mis-match of yield strength of the constituent parent and weld metals, strong gradients of material properties due to the transition in metallurgical structure, the presence of welding residual stresses and mixed mode loading of the defect.

ADIMEW (Assessment of Aged Piping Dissimilar Metal Weld Integrity) was a three-year collaborative research programme carried out under the EC 5th Framework Programme (Ref. 1). The objective of the study was to advance the understanding of the behaviour and safety assessment of defects in DMWs representative of those found in nuclear power plant. Several European organisations participated in the ADIMEW project including: EDF (Project Co-ordinator), CEA, Framatome, JRC-IAM Petten, Serco Assurance, TWI, VTT and the Bay Zoltán Institute.

[1] john.wintle@twi.co.uk (corresponding author)
[2] bridget.hayes@twi.co.uk
[3] martin.goldthorpe@twi.co.uk

The ADIMEW project studied and compared different methods for predicting the behaviour of defects located near the fusion boundaries of DMWs typically used to join sections of austenitic and ferritic piping operating at high temperature. The study included the measurement of material properties and residual stresses, predictive engineering analysis and validation by means of a large-scale test.

The ADIMEW participants used a range of techniques to predict the outcome of the tests. These included conventional analysis methods such as the *J*–integral approach, the SINTAP assessment procedure (Ref. 2) and more advanced techniques using micro-mechanical models of material failure.

This paper presents the results of TWI contributions to ADIMEW including: fracture toughness testing of the buttering, weld and Heat Affected Zone (HAZ) constituents of the DMW; residual stress measurements; and assessments of the ADIMEW test using three-dimensional, elastic-plastic, cracked body, finite element analysis.

ADIMEW TEST ASSEMBLY, DEFECT CONFIGURATION AND LOADING

Test assembly

The overall geometry of the ADIMEW test specimen is illustrated in Figure 1. The central test section consisted of two approximately 0.5 m long cylinders, each welded to a 4 m extension arm of high strength steel. These arms were used to apply a bending moment to the test section.

In the central test section of the assembly, a 453 mm external diameter and 51 mm thick section of type A508 Class 3 ferritic pipe was joined to a similar section of type 316L austenitic pipe. This attachment used a type 308L austenitic steel girth weld with a 'V' preparation inclined at 25° to the normal to the pipe axis (Figure 2). The weld 'mock-up' was post-weld heat-treated for four hours at 610°C.

Two dissimilar metal weld mock-ups were manufactured within the programme. The first, AD01, was cut-up to measure welding residual stresses and provide small-scale specimens for measurement of tensile and fracture toughness properties of the constituent parent steels, weld metals and associated heat affected zones. The second mock-up, AD02, was used for the actual test.

Defect Configuration

As illustrated in Figure 3, in weld mock-up AD02 a circumferential, surface-breaking, planar defect was inserted into the type 309L/308L buttering layer between the main weld and the ferritic base material by means of electro-discharge machining (EDM). The plane of the defect was parallel to the local fusion line and so inclined at 25° to the normal to the pipe axis. The front of the defect was straight and lay within the layer of weld buttering at an axial distance of about 1.5 mm from the fusion line between the buttering and the A508 pipe. The maximum depth of the defect (a_{max}) was 17 mm, measured normal to the pipe axis, or 18.76 mm measured from the middle of the defect mouth to the middle of the straight defect front. The various dimensions and angles associated with the defect are given in Figure 3.

Loading

As shown in Figure 4, the test assembly was subjected to four-point bending in order to promote ductile tearing of the defect, with the ferritic and austenitic sections of interest in the mock-up held at a temperature close to 300°C. The test assembly was positioned in the loading rig to give equal ram displacements and loads on either side of the mock-up.

R-CURVE FRACTURE TOUGHNESS TESTING

Scope of testing and test matrix

After some changes to the programme, TWI carried out a series of tests at 300°C to determine the ductile fracture toughness of the constituent materials around the dissimilar metal weld and the location of the test defect. Table 1 shows the test matrix and gives the identity numbers of the specimens.

The test specimens were taken from the AD01 weld mock-up. Two blocks of material containing a length of the dissimilar metal weld were supplied for the tests as follows:

- the window initially cut out of assembly AD01 (used for the first six tests in Table 1),
- an arc after AD01 had been later sectioned and cut up (used for the final six tests in Table 1).

Specimen preparation and testing procedure

All specimens were designed and prepared according to the requirements of BS 7448 (Ref. 3). Specimens were cut from blocks supplied. Notches were cut into the specimens by EDM, and then the specimens were fatigue pre-cracked.

In specimens A2-1 and A2-2 the fatigue crack growth deviated from the line of the notch at an angle of 25° to 30°, veering away from the fusion line and further into the buttering. This amount is beyond that specified in BS 7448 for a valid specimen. The ADIMEW consortium discussed the best course of action and decided to side-groove the specimens from the tips of the deviated fatigue cracks in order to increase crack tip constraint. The unloading compliance fracture tests would be performed and analysed according to standard; even though the cracks were inclined to the principal axial bending stress. However, the validity of the results would be questionable. It was also agreed that, in order to grow a straight fatigue pre-crack, a procedure devised by Framatome should be followed in which a shallow side-grooves are machined before fatigue pre-cracking and then deepened when pre-cracking is complete. A procedure given by GKSS and EdF was also adopted for the preparation of the other specimens in order to limit the maximum force for pre-cracking. Fatigue pre-cracking proceeded in two steps at different R ratios (0.1 and 0.7) in order to obtain a uniform crack front.

Test analysis

The measurements made during the tests were analysed using the method given in the standard BS 7448:Part 4 to determine crack growth resistance curves in terms of J. This method is intended to apply to specimens with homogeneous properties; whereas the ADIMEW specimens involve a combination of materials with distinctly different stress-strain properties and Young's moduli.

'Eta' factors: The value of the η ('eta') factor that should be used in the computation of J for the ADIMEW dissimilar metal weld specimens is a matter for on-going discussion. A η factor of 2.0 was used in the computation of the plastic component of J, which is the value given in the standard as appropriate to homogeneous single edge-notch bend (SENB) specimens. η factors for mismatched welds (between common parent material) have been discussed in a number of papers during the past few years. In Ref. 4, the η factor was shown to be dependent on the weld strength mismatch value, as well as the width of the weld and size of the uncracked ligament. In Ref. 5, Kirk and Dodds give a formula for η for mismatched SENB specimens; stated to hold when the mismatch ratio of yield strengths lies between 0.5 and 1.3. For a crack depth to width ratio of 0.5 the η factor predicted by Ref. 5 is 2.7 compared with a value of 2.0 for a homogenous specimen.

Blunting line: To determine J at initiation of ductile tearing, a blunting line was used in accordance with BS 7448 Part 4. The line has a slope of $3.75R_m$ where R_m is the tensile strength of the material around the crack tip at the test temperature, and intersects the crack growth axis at $\Delta a = 0.2$ mm. A value of R_m of 441 MPa was used in the analysis of the BU_{FL}, FL_{BU} and weld metal tests and 640 MPa for the CGHAZ test.

Resistance curves: The J versus Δa data for each test were processed to obtain best-fit curves through the range of valid points according to BS 7448:Part 4. These were taken to be those points lying between the lines parallel to the blunting

lines drawn through 0.1 mm and Δa_{max} (10% of the ligament). A few data points that clearly did not form part of the general population were excluded. A power law curve of the form $J=m+L(\Delta a)^x$ was fitted to the valid data points of each test.[4]

Results for the buttering layer

The *J*-R curve data for the specimens sampling the buttering layer are plotted together in Figure 5. Filled symbols denote valid data, and open symbols are beyond the Δa validity limit. The curves fitted to the data within the Δa limits are shown in the figure. Each curve has been extrapolated to indicate the trend. Table 2 lists the parameters m, L and x of the curve fit. In most cases the intercept m was negative and therefore not strictly valid according to BS 7448:Part 4. This table also shows for each test the initiation of stable crack growth, as defined by $J_{0.2}$, and gives the J obtained from the fitted curves for different amounts of growth. As the curves were fitted only to valid data, they may not always fit the non-valid data. Extrapolation to larger amounts of growth is therefore only indicative of the values that might be achieved.

Discussion of fracture toughness results

The use of 20 mm x 40 mm specimens therefore allows valid *J*- R curves to be generated for crack growth up to 1.75 mm as opposed to less than 0.5 mm for the 10 mm x 10 mm specimens. The data from the two sizes of specimen is consistent up to Δa of about 1 mm, with the larger specimens (W01-04 and W01-05) showing a flattening R-curve at larger amounts of growth.

The main feature of these results suggests that the buttering material on and near the fusion line of the ADIMEW dissimilar metal weld has a low $J_{0.2}$ initiation toughness and a low resistance to tearing. These are significantly lower than those of the bulk weld metal or the coarse grain heat affected zone (CGHAZ). The appearance of such good properties for the CGHAZ is a little surprising, since a martensitic structure would normally be expected and have the lowest properties. Low heat input weld deposition of the buttering or a variation of microstructure away from the fusion face might explain the results, but for a definitive answer further examination of the material is required. The buttering material on and near the fusion line is therefore the weld material with the lowest resistance to fracture.

The $J_{0.2}$ obtained (53/58 kJ/m^2 from 10 mm x 10 mm specimens and 59/63 kJ/m^2 from 20 mm x 40 mm specimens) are significantly lower than that of 130 kJ/m^2 obtained for equivalent buttering material at 20°C in the previous BIMET project (Ref. 6). These results are also lower than the values ADIMEW partners Framatome and the Bay Zoltán Institute obtained from compact tension (CT) specimen tests of the ADIMEW weld, although these tests also indicated a flat R-curve and comparable values at larger amounts of growth (look ahead to Figure 9, the curve labelled 'ADIMEW, power law fit 4').

The reasons for the difference between ADIMEW and BIMET results are not entirely clear. The ADIMEW and BIMET welds were produced by different fabricators, although they were of comparable specification. Any differences in the detail of the welding procedure, consumables, thickness and heat treatment could be relevant. Examination of the relevant microstructures of the BIMET and ADIMEW welds could determine if there were any significant differences between the weld materials.

Reasons for the differences with the Framatome and Bay Zoltán compact tension data are probably a result of differences in the notch and crack growth path. In the two single-specimen Framatome CT tests, the ductile crack growth deviated out of the side-groove and exhibited considerable tunnelling with the centre of the crack running well in advance of the edges. Both of these effects would tend to result in an overestimate of J compared with the present tests. In addition, Framatome used a blunting line with a slope of 4 times the flow stress, giving a slightly lower slope than the $3.75R_m$ value that TWI used, and hence a larger value of $J_{0.2}$.

The Bay Zoltán CT tests were undertaken on specimens with electro-discharged machined notches without fatigue pre-cracking; similar to the notch cut into the ADIMEW full-size test weld. A higher value of $J_{0.2}$ relative to that obtained from fatigue pre-cracked specimens was therefore expected and observed. The Bay Zoltán tests also showed some sensitivity of

[4] In the fracture mechanics assesments described later some fits were made including data invalid according to BS 7448.

the R-curve to the distance of the notch from the fusion line; with the toughness decreasing as the fusion line was approached on the buttering side. Differences in the positioning of the starter notch and fatigue pre-crack between the different laboratories could therefore also be a factor in explaining the differences between the *J*-R curves obtained.

As seen later in the later description of the fracture mechanics assessment, these and other fits to 'all-valid' and 'both valid and invalid' fracture toughness test results are used to predict the outcome of the ADIMEW test. Of course, it is highly dubious to use extrapolated fracture toughness for very extensive amounts of tearing well beyond the range and validity of the test measurements. Nevertheless, such extrapolation has to be done in order to carry out a full fracture mechanics assessment of the large-scale test.

RESIDUAL STRESS MEASUREMENTS BY HOLE DRILLING

Method

TWI undertook measurements of residual stresses across the dissimilar metal weld in the AD01 pipe assembly. This used the surface hole drilling method (Ref. 7). The hole drilling method is a standard method for measuring residual stresses close to a free surface. It uses three strain gauges positioned around the location to be measured. They are conventionally aligned parallel and perpendicular to the principal axes of the component and at an angle of 135°. A small hole of approximately 2.1 mm diameter is made in the surface at the location to be measured using a fine abrasive powder jet. As the hole deepens, a change in surface strain is recorded on the gauges. When the hole depth has reached about 2 mm, the jet is stopped and the final readings of the strain gauges are recorded. The strain and hole size measurements recorded at each location allow the calculations of in-plane principal stresses and orientation angle. These are resolved to determine the stresses in the directions parallel and circumferential to the pipe axis. The accuracy of residual stress measurement by the centre hole method is claimed to be ±8% for stresses up to 65% of yield.

Residual stress results and discussion

The results for axial surface residual stresses on the outside and inside of the pipe are shown in Figure 6 and Figure 7, respectively. These measurements suggest that the axial surface residual stresses are compressive. These residual stresses would tend to have a closing effect rather than causing additional opening of the defect in the ADIMEW test pipe.

This appearance of compressive stresses is somewhat unexpected; since tensile welding residual stresses usually occur on the outside of similar, as-welded girth welds in (homogeneous) stainless steel pipes, Ref. 8. However, there is much variability in the experimental results given in Ref. 8, depending on factors such as pipe geometry, weld preparation and welding heat input. It should also be remembered that the ADIMEW pipe assembly concerned a dissimilar metal weld. In addition, the ADIMEW weld was post-weld heat treated at 600°C for six hours and subsequently machined on the outside surface. These operations would have altered the residual stress from the stresses in the as-welded condition.

The TWI results show considerable discrepancy in comparison with the volumetric residual stress measurements that the Joint Research Centre (JRC) Petten made using neutron radiography, and the finite element calculations made by Framatome for the ADIMEW test weld AD01. However, there is reasonable agreement with measurements made by the MarTec Laboratory in Switzerland using the block splitting technique, Ref. 9. These measurements show that the compressive stress on the surfaces is a purely local effect. Beneath the surfaces the stresses revert to those consistent with measurements made by JRC and calculated by Framatome. The volumetric sensitivity of neutron radiography measurements and finite element calculations would not have been capable of identifying a local stress within a few millimetres of the surface. The compressive stress on the surfaces is probably a result of the machining that was carried out after post-weld heat treatment. There is some experimental evidence to support this view, for example Ref. 10, but a lack of data for materials and conditions that are truly representative of the ADIMEW test pipe. As the effect of compressive surface residual stress would be to inhibit the initiation of surface cracking from corrosion, further study of residual stresses close to machined surfaces could be beneficial.

FRACTURE MECHANICS ASSESSMENT USING FINITE ELEMENT ANALYSIS

Material properties

Tensile properties: VTT measured tensile properties of the various constituents of the weld mock-up using specimens cut out of the mock-up AD01. Figure 8 shows the true stress versus true strain behaviour of the different materials comprising the mock-up at the 300°C test temperature. Table 3 summarises the main tensile properties as used in the finite element analyses. Type 308L weld properties were used for the buttering.

Fracture toughness resistance curves: Fracture toughness versus ductile tearing resistance curves were measured for the weld buttering layer by ADIMEW participants as well as TWI. Figure 9 shows five different *J*-R curve fits. They are in descending order:

- 'ADIMEW, power law fit 1' is an early fit to valid data only for TWI specimen A2-2(M02-02) at 300°C discussed above;
- 'BIMET, power law fit' is the consensus fit for the buttering layer used in the BIMET project at 20°C (Ref. 6);
- 'ADIMEW, power law fit 2' is an approximate fit to both valid and invalid data for TWI specimen A2-2(M02-02) at 300°C;
- 'ADIMEW, power law fit 4' is a fit to the results from the blunt notch CT specimen no. 1 tested by the Bay Zoltán Institute at 300°C;
- 'ADIMEW, power law fit 3' is a fit to valid data for the TWI 20x40 mm SENB specimen W01-05 at 300°C discussed above.

With the exception of ADIMEW fit 1, all the fits show relatively shallow *J*-resistance curves, with varying levels of initiation toughness, $J_{0.2}$; the highest associated with the fit to data from the blunt notch CT specimen, ADIMEW fit 4.

Finite element analyses

The computations were carried out using Version 5.8 of the ABAQUS finite element program (Ref. 11).

Meshes: Eight different meshes were set up having the following values of maximum crack depth, a_{max}: 17, 18, 19, 20, 21, 22, 24 and 26 mm. Figure 10 shows an overall view of the ADIMEW test pipe mesh, with the loading and reaction positions indicated. Only one half of the test assembly was modelled on one side of the vertical plane of symmetry. The defect is at the 12 o'clock position at the top of the pipe. There are 28,048 elements in the entire mesh with ABAQUS elements type C3D8H used throughout. This is an 8-noded, first order, three-dimensional, hybrid element that is suitable for modelling large-scale plastic deformation. The bevelled, dissimilar metal weld in the neighbourhood of the defect is clearly seen in Figure 11.

Figure 12 shows two pictures relating to the defect itself. The left-hand picture shows the focused mesh surrounding the crack front, where the latter intersects the plane of symmetry. The dashed white line denotes where the coincident crack flanks meet the vertical symmetry plane of the pipe. There are 12 rings of elements in the square section box surrounding the crack front, with 32 elements around each ring. The innermost rings of elements immediately adjacent to the crack front are standard type C3D8H but each has one face collapsed onto the local segment of the crack front. The right-hand picture in Figure 12 shows only weld metal elements on the austenitic side of the defect plane. Dashed lines indicate the boundary of the defect. A total of 12 equal length segments, and so 12 elements lengths, are used along the half-length crack front modelled in the mesh. There are 13 nodal positions along the crack front; the drawing points out the nodes labelled 'J_{11}' at the middle of the crack front (at the vertical plane of symmetry) and 'J_{23}' where the crack front meets the outer pipe surface.

Boundary and loading conditions: The nodes on the vertical plane of symmetry were constrained appropriately. The vertical component of displacement was restrained at each of the two nodes positioned at the restraint points 7 m apart (Figure 4, Figure 10). At the two nodes positioned at the loading points 3 m apart, an equal vertical displacement was

imposed in order to simulate the loading rams. To ensure equal loading of the two rams, the centre-line of the loading arrangement (Figure 4, Figure 10) was offset an axial distance d=275 mm from the crack mouth into the austenitic pipe. During initial pre-test calculations, it was discovered that the balance of load on the rams was very sensitive to the precise value of the offset d.

The entire mock-up was assumed to be at a uniform temperature of 300°C. Any welding residual stress remaining after stress-relief was ignored.

Small strain, elastic-plastic, analyses were carried out, with the first loading step of each consisting of a relatively low value of ram displacement of 0.1 mm thus giving predominantly elastic response. In all eight analyses, the remainder of the 250 mm maximum ram displacement was imposed in 25 equal increments.

Finite element fracture mechanics analysis results

This section describes the main fracture mechanics results from the 8 cases of a_{max} studied by finite element analysis, combined with the various J-R curve fits considered for the weld buttering.

Elastic solutions: Using the initial elastic solution for each defect depth, the local mode I stress intensity factor, K_I was evaluated at each of the 13 nodal positions on the (half length of the) crack front as follows:

$$K_I = \left(\frac{J_{el} E}{(1-\nu^2)} \right)^{1/2}$$

where J_{el} is the local elastic component of the J-integral calculated assuming co-planar virtual advance of the crack, and E and ν are the Young's modulus and Poisson's ratio of the 308L weld metal. The stress intensity factor K_I is normalized by K_o, given by

$$K_o = \sigma_b (\pi a_{\max})^{1/2}$$

where the bending stress σ_b is given

$$\sigma_b = \frac{4Mr_0}{\pi(r_o^4 - r_i^4)}$$

where M is the applied bending moment at the cracked section of the pipe and a_{max}, r_i and r_o are defined in Figure 3.

Figure 13 presents such results for K_I/K_o versus distance from the middle of crack front normalized by the half length of the front, c. These normalised stress intensity factors have peak magnitudes as expected (peak values between 1.1 and 1.2), increase with maximum crack depth and decrease from the middle of the front towards the free surface.

Elastic-plastic solutions, initiation predictions: Figure 14 gives predictions of elastic-plastic J versus applied bending moment at the cracked section for the initial ADIMEW crack configuration, with a_{max}=17 mm. Curves of results are shown for every 2nd node along the half length of crack front modelled. As noted earlier, node 'J_{11}' is at the middle of the crack front and 'J_{23}' is where the crack front intersects the outside of the pipe. This figure also shows a series of horizontal lines showing the level of $J_{0.2}$ initiation toughness for the five different fits considered for the weld buttering. The range of moment required to cause initiation is rather wide.

Table 4 summarises results for bending moment required to cause initiation of ductile crack growth at the middle of the crack front. This also includes the crack mouth opening displacement (CMOD) measured at the centre of the crack mouth. The estimated value of bending moment at initiation in the ADIMEW test, based on electric potential drop measurements, was about 1.91 MN m. This result is consistent with predictions made using 'fit 4' based on the Bay Zoltán blunt notch CT specimens of ADIMEW buttering material tested at 300°C. This is not surprising since the defect in the ADIMEW test was also cut by EDM and so blunt. Predictions of initiation moment, based on J-R curve fits to tests on fatigue pre-cracked specimens, are not surprisingly lower.

Tearing predictions: Figure 15 compares two of the considered fracture toughness resistance curves, for an initial 17 mm maximum crack depth, with applied or driving force curves of J versus maximum crack depth for four different values of constant bending moment. These are given in the legend. The 'BIMET' and 'ADIMEW fit 2' resistance curves achieve tangency with the curves of applied J, and so reach a maximum bending moment, after about 22 mm and 25 mm of tearing, respectively. Of course, it is assumed here that the front of the defect tears in a uniform manner. This is obviously an approximation considering the variation of driving force along the front seen Figure 13 and Figure 14. It is apparent from Figure 15 that maximum bending moment is slightly greater than 2 MN m for these two J-R curves.

Again assuming uniform tearing along the front, Figure 16 uses the finite element results for applied J, plus the material J-R curve fits, to predict bending moment at the cracked section versus crack depth for all five J-R curves considered. The 'ADIMEW fit 1' resistance curve predicts a maximum moment in excess of 2.45 MN m at a_{max} somewhat greater than 26 mm (more than 9 mm tearing). The corresponding figures for the BIMET material fit are 2.09 MN m at a_{max}=21.40 mm (4.4 mm tearing). ADIMEW fit 2 gives a maximum moment of 2.04 MN m at a_{max}=23.8 mm, that is, after 6.8 mm of tearing. ADIMEW fit 4 predicts a maximum moment of nearly 2 MN m, but the moment versus crack depth curve is not well rounded due to lack of smoothing of the J-Δa relationship near initiation. The predicted moment versus crack depth curve from ADIMEW fit 3 is the lowest of all.

It is very noticeable that most of these predictions give broad plateaux and the plastic yield moment is relatively insensitive to crack depth for the range of a_{max} considered. Tearing and stability of the defect are therefore controlled primarily by the flat tearing resistance of the buttering material, and the rapid change in applied J with bending moment above about 1.8 MN m, with little interaction with the applied load. It should be noted that gross yielding of the pipe assembly occurs mainly in the 316L parent pipe; away from the location of the defect.

Figure 17 shows predictions of bending moment versus CMOD for the five resistance curves. According to the ADIMEW fit 2 the bending moment peaks at 2.04 MN m when the CMOD is about 2.35 mm, though again the plateau is broad. For comparison, Figure 18 shows a corresponding set of results from the test. The agreement between ADIMEW fit 2 predictions (using fit to valid and invalid SENB specimen tests) and the large-scale test result itself is remarkably good. (That 'fit 4' best predicts initiation while 'fit 2' best predicts the growth behaviour is not surprising. 'Fit 4' was based on a blunt notch (as in the test), whereas 'fit 2' has more data at larger amounts of tearing.)

Estimates were made of the crack growth profile using the finite element results in conjunction with the 'ADIMEW fit 2' fracture toughness versus crack growth relationship. These are shown in Figure 19. The estimated amount of crack growth at each of the 13 nodes on the half-length of the crack front modelled is shown against normalised distance from the middle of the crack front. Curves are shown for different applied bending moments. Crack growth is estimated at each node by matching the applied crack driving force for a given crack depth, $J_{app}(M, a= a_o+\Delta a)$, with the increasing material fracture toughness $J_{mat}(\Delta a)$. Here a_o is the initial crack depth at each node based on the initial a_{max}=17 mm. Of course, these profiles are approximate estimates because the crack driving force values are based on the finite element analyses modelling a straight crack front; rather than the proper developing curved front. The decreasing steps in moment, moving up the legend of Figure 19, demonstrate an increasing sensitivity of crack growth to bending moment as growth proceeds. Of course, results are limited to maximum crack growth less than 9 mm, since the largest a_{max} considered in the analyses is 26 mm. These predictions suggest that no crack growth takes place at the free surface.

DISCUSSION

The actual ADIMEW pipe test showed a substantial amount of ductile crack growth of the initial defect, a maximum of 28.1 mm through the wall of the pipe, but with no change to its circumferential length around the pipe, as illustrated in Figure 20. This suggests potential for leak-before-break rather than a guillotine failure. The test is therefore a demonstration that supports safety.

Such large extent of tearing observed in the test should not be treated with undue alarm; it is a consequence of the maximum ram displacement applied. The bending moments required for significant growth of the defect are close to those required for plastic yielding or collapse of the uncracked pipe. The defect makes negligible difference to structural behaviour of the pipe as a whole. Moments of this magnitude would not be expected to occur during normal operation of such pipework in real plant.

Pre-test discussions and studies envisaged that tearing would be limited to about 9 mm: this led to the maximum 26 mm crack depth (i.e. 17 mm initial plus 9 mm tearing) considered in this study. Crack behaviour up to about 9 mm of tearing was successfully predicted by finite element *J*-based methods. Bending moments for initiation and maximum load were approximately correct and support the use of such analysis.

The toughness of the mock-up buttering layer as measured by small specimens appears to be consistent with a fairly shallow resistance curve. The flat moment versus crack depth or CMOD curves determined in the test reflect the shallow resistance curve of the buttering material. There is therefore potential for large amount of stable tearing if the loads applied are sufficient. The microstructural and mechanistic reasons for the flat R curve behaviour are not entirely clear at present.

The cracked section of the pipe is subjected to a predominantly tensile stress field. This may impose less plastic constraint ahead of the crack front than the side-grooved three-point bend and compact tension specimens used to provide the various *J*-R curves. This difference in crack tip plastic constraint can lead to higher values of apparent fracture toughness in the ADIMEW test pipe geometry: see for example Ref. 12. These higher values of toughness would give less extensive ductile tearing than predicted here at a particular measured value of a test parameter such as bending moment or CMOD.

However, the test results obviously do not bear this out. The apparent toughness of the buttering appears to be consistent with a shallow resistance curve extrapolated from both valid and invalid test results on deeply-cracked (albeit small) bend specimens. It is therefore important to find out, in any future studies of the ADIMEW test, why there appears to be no benefit or margin conferred by structural constraint. One reason could be the confinement of the crack tip plastic zone by the high yield strength ferritic parent pipe; despite gross yielding taking place in the uncracked 316L pipe. More work on this subject linking the microstructure of the buttering layer to the crack tip plastic zone would be worthwhile.

CONCLUSIONS

1. Buttering material on and near the fusion line of the ADIMEW dissimilar metal weld has a low $J_{0.2}$ initiation toughness, and a low resistance to tearing, as measured using fatigue pre-cracked specimens. These are significantly lower than those of the bulk weld metal or the coarse grain heat affected zone.
2. Axial residual stress across the dissimilar metal weld is predominantly compressive on both the inside and outside surfaces of the pipe. This is probably a result of the machining that was carried out after post-weld heat treatment. The block splitting technique shows that beneath the pipe surfaces the stresses revert to those consistent with measurements made by JRC and calculated by Framatome.
3. *J*-based finite element analysis successfully modelled the macroscopic deformation and fracture behaviour of the ADIMEW test pipe.
4. The analysis could predict the load at initiation of ductile tearing accurately, but the prediction was critically dependent on the degree of representation of the resistance curve derived from the small-scale fracture test to that the full size test pipe in terms of crack sharpness, material microstructure and possibly constraint.
5. The analysis successfully predicted the narrow range of load over which significant growth of the defect occurred; a consequence of the low tearing resistance of the buttering material and the rapid change in applied J with bending moment above about 1.8 MN m.
6. The observed growth of the defect through the wall, but without change in circumferential extent, was successfully predicted from the analysis results, suggesting potential for leak-before-break rather than a guillotine failure

ACKNOWLEDGMENTS

The authors acknowledge the useful collaboration with other ADIMEW partners. They are also grateful for financial support from DG XII of the CEC, under the 5th Framework Programme, and from UK Health and Safety Executive and IMC.

REFERENCES

1. Faidy et al, The ADIMEW Project, Proceedings FISA Conference 2003.
2. 'Structural Assessments Procedure for European Industry (SINTAP)', November 1999.
3. BS 7448-4:1997, 'Fracture mechanics toughness tests. Method for determination of fracture resistance curves and initiation values for stable crack extension in metallic materials'.
4. Wardle G: 'Evaluation of Fracture Toughness and Fatigue Crack Growth for Transition Welds at Non-Creep Temperatures', AEA Technology report AEAT-4263 for European Commission contract B7-5340/96/000792/MAR/C2, July 2000, Vaidya W V et al: Tasks 1c and 1f: Methods used to determine fracture toughness values and recommendations for specific procedures to be used for transition welds', GKSS Document No.: P3203F02#3, September 1998.
5. Kirk M T and Dodds R H: 'J and CTOD estimation for shallow cracks in single edge notched bend specimens', *Journal of Testing and Evaluation*, Vol 21, No 4, 1993.
6. Chas G, Faidy C and Hurst R C: "Structural integrity of bi-metallic components program (BIMET): fracture testing of bi-metallic welds, Paper 8585, Proceedings of ICONE 8, April 2-6, 2000, Baltimore USA.
7. Beaney E M: 'Accurate measurement of residual stress on any steel using the centre hole method'. *Strain* 9999-106, April 1976.
8. Bouchard P J and Bradford R A W: 'Validated axial residual stress profiles for fracture assessment of austenitic stainless steel pipe girth welds', PVP Vol. 422: Fracture and Fitness, Proceedings of ASME PVP Conference, Atlanta, Georgia, USA, July 22-26, 2001.
9. Schindler H J: 'Residual stress effects on crack growth mechanisms and structural integrity', 9th Conf. on Mechanical Behaviour of Materials, Geneva, Switzerland, 25-29, May 2003.
10. Leggatt R H, Scaramangas A A and Porter Goff R F D: 'On the correction of residual stress measurements obtained using the centre hole method'. *Strain*, pp.88-96, August 1982.
11. ABAQUS/Standard User's Manuals, Version 5.8. Hibbitt, Karlsson and Sorenson Inc., 1080 Main Street, Pawtucket, Rhode Island, USA, 1998.
12. Anderson T L and Dodds R H: 'A framework for predicting constraint effects in shallow notched specimens'. *Proceedings of the International Conference on Shallow Crack Fracture Mechanics Tests and Applications*, held at TWI, Cambridge, 23-24 September 1992.

Specimen type	Dimensions B, W, L Mm	Notch location	Temp °C	Number of tests	Type of test	Specimen identity
SENB BxB sub size	10, 10, 55	BU_{FL}	300	3	J_R unloading compliance	A2-1(M02-01) A2-2(M02-02) A3-3(M02-03)
SENB sub size	10, 10, 55	FL_{BU}	300	2	J_R unloading compliance	A2-3 A3-1
SENB sub size	10, 10, 55	CGHAZ	300	1	J_R unloading compliance	A3-2
SENB Sub size	10, 10, 55	WM	300	3	J_R unloading compliance	W01-01 W01-02 W01-03
SENB Bx2B B=20 mm	20, 40, 100	BU_{FL}	300	3	J_R unloading compliance	W01-04 W01-05 W01-06

where:
BU_{FL} indicates the notch is located in the weld buttering 1-2 mm from the fusion line,
FL_{BU} indicates the notch is located on the fusion line tending towards the buttering side,
CGHAZ indicates the notch is located in the coarse grained heat affected zone,
WM indicates that the notch is located in the bulk weld metal.
The notch direction is parallel to the fusion line in all cases.

Table 1: Fracture toughness testing matrix

Specimen identity	Notch location	m	L	x	$J_{0.2}$	$J_{0.5}$	$J_{1.0}$	$J_{2.0}$
A2-2(M02-02)	BU_{FL}	-6.6	+186.0	0.73	58	106	179	302
A3-3(M02-03)	BU_{FL}	-0.2	+232.1	1.00	53	116	232	464
W01-04	BU_{FL}	+16.3	+188.1	0.58	63	110	172	265
W01-05	BU_{FL}	-902.9	+1055.2	0.06	59	109	152	197

Table 2: J versus ductile tearing Δa curve fits for buttering layer: $J=m+L(\Delta a)^x$, with J in kJ/m^2, Δa in mm

Material	Elastic Modulus, E, MPa	Poisson's Ratio, ν	Limit of proportionality, σ_y MPa	0.2% proof stress, $\sigma_{0.2}$, MPa
A508 parent and HAZ (300°C)	231500	0.3	367	463
308L weld and buttering (300°C)	167500	0.3	161	335
316L parent (300°C)	106500	0.3	151	213
carbon steel arms (20°C)	208000	0.3	N/A	N/A

Table 3: Material tensile properties used in the finite element analysis

J-R curve	$J_{0.2}$ (kJ/m^2)	Moment, M, (MN m)	CMOD (mm)
ADIMEW, power law fit 1 to valid data only, 300°C	43.7	1.470	0.304
BIMET, power law fit, 20°C	130.4	1.804	0.695
ADIMEW, power law fit 2 to all test data, 300°C	48.4	1.502	0.329
ADIMEW, power law fit 4, 300°C	235.0	1.980	1.080
ADIMEW, power law fit 3 to valid data only, 300°C	55.2	1.549	0.365

Table 4: Summary of predictions of ADIMEW crack initiation moment and CMOD (giving 0.2 mm ductile tearing at middle of crack front); estimate of moment at initiation during test itself is 1.85 MN m

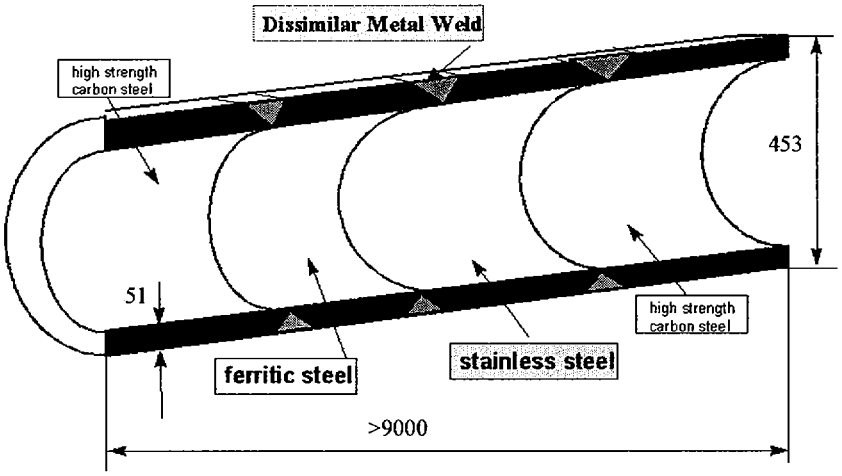

Figure 1: Schematic of overall geometry of ADIMEW test specimen

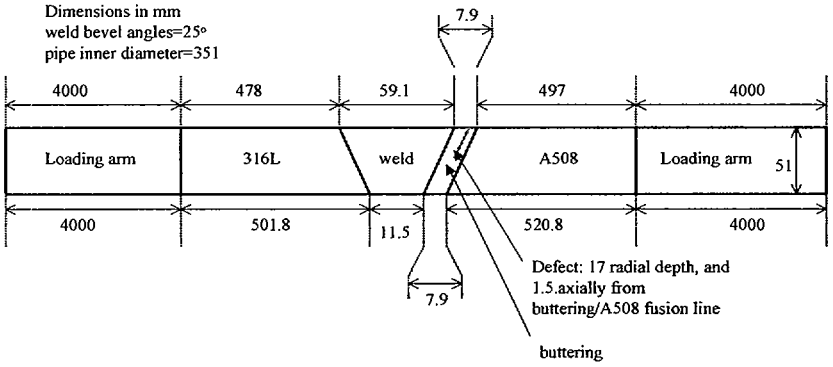

Figure 2: Section through the test specimen (not to scale) showing the various materials and main dimensions

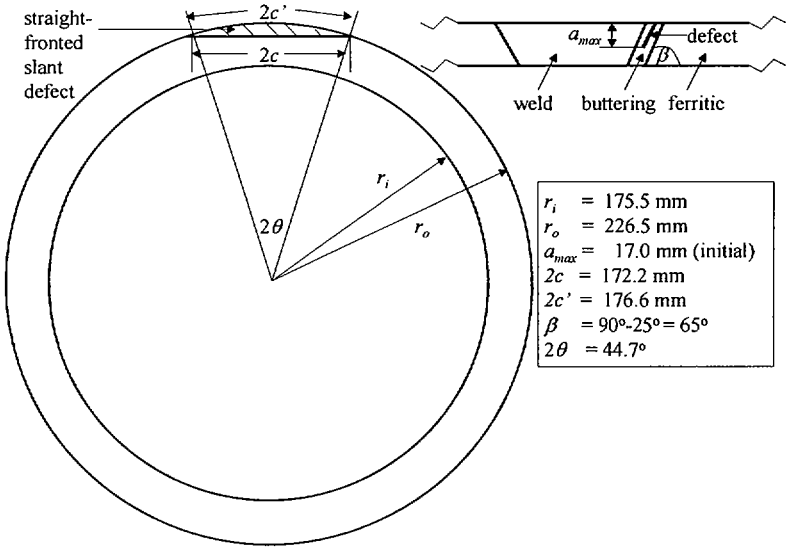

Figure 3: Geometry of defect in ADIMEW test specimen showing associated dimensions

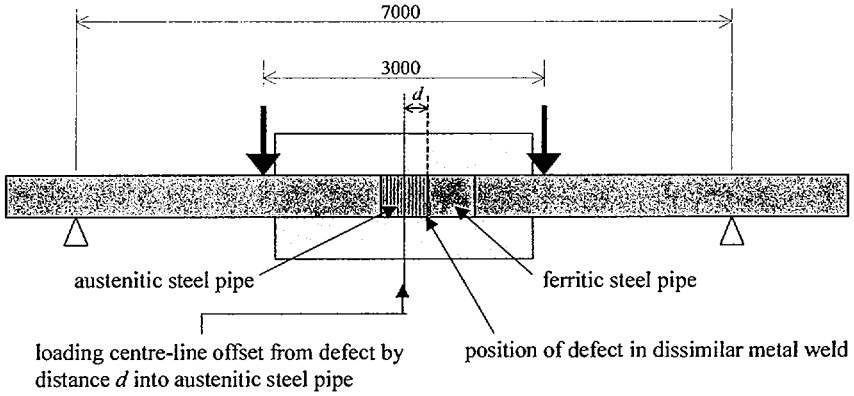

Figure 4: Four-point bending loading configuration of ADIMEW test assembly

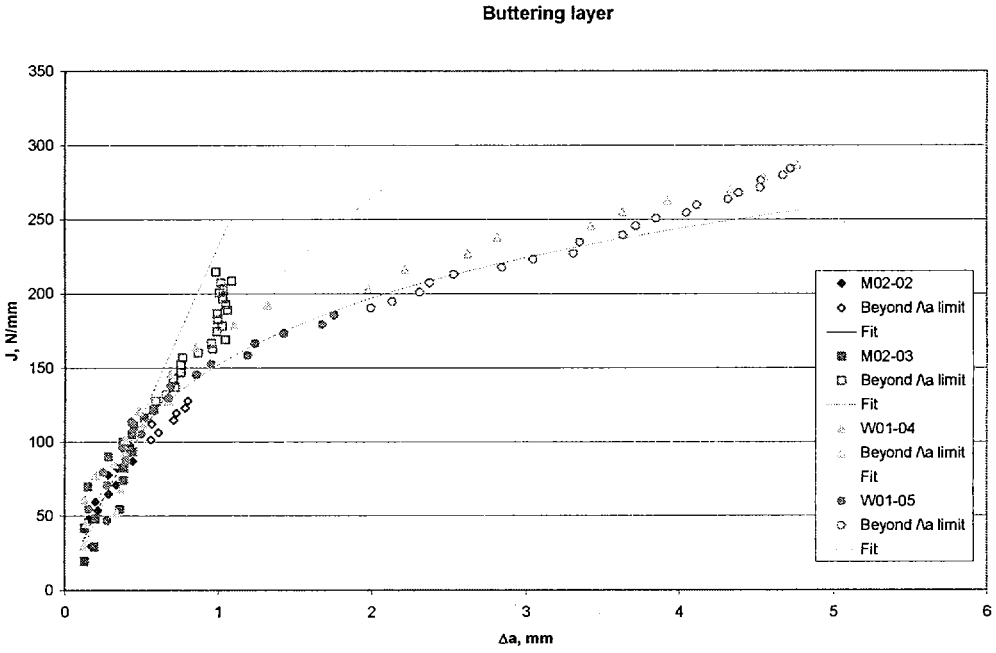

Figure 5: *J*-R curves obtained for the buttering layer

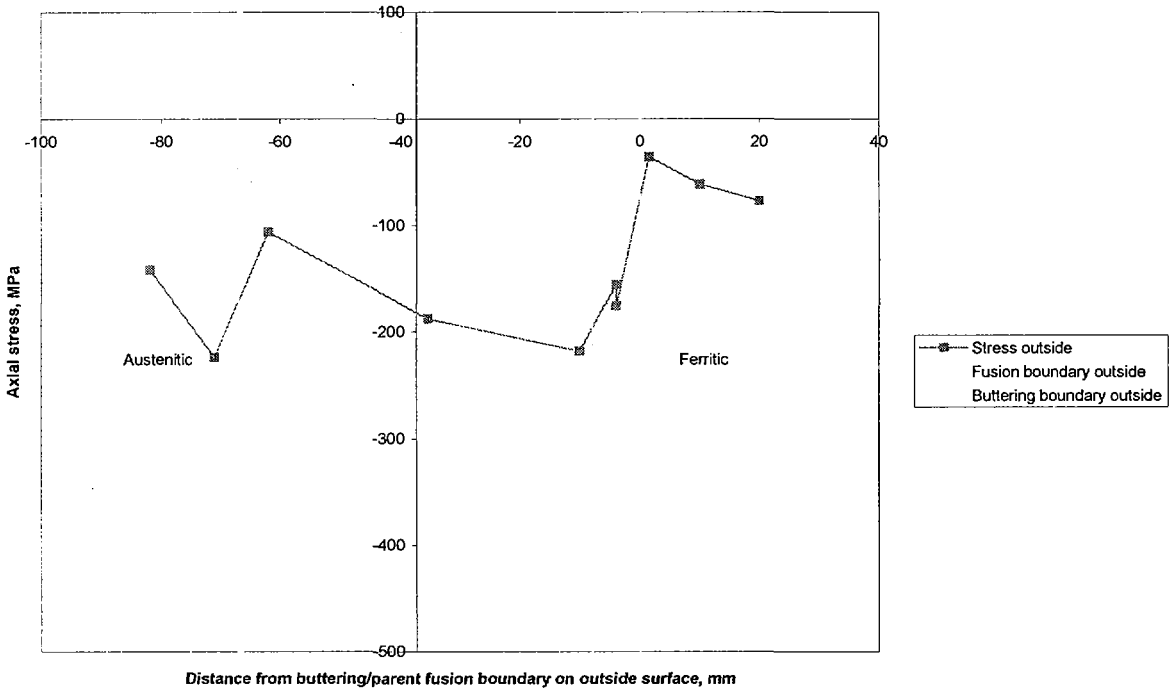

Figure 6: Axial residual surface stresses on outside of pipe measured across dissimilar metal weld

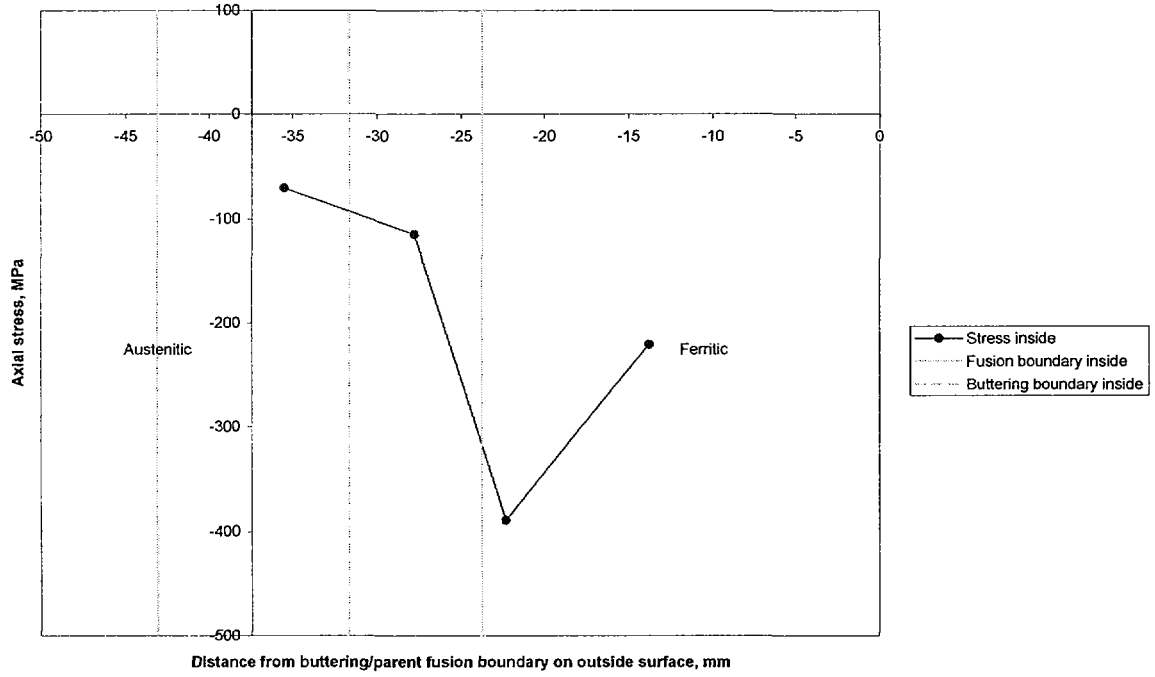

Figure 7: Axial residual surface stresses on inside of pipe measured across dissimilar metal weld

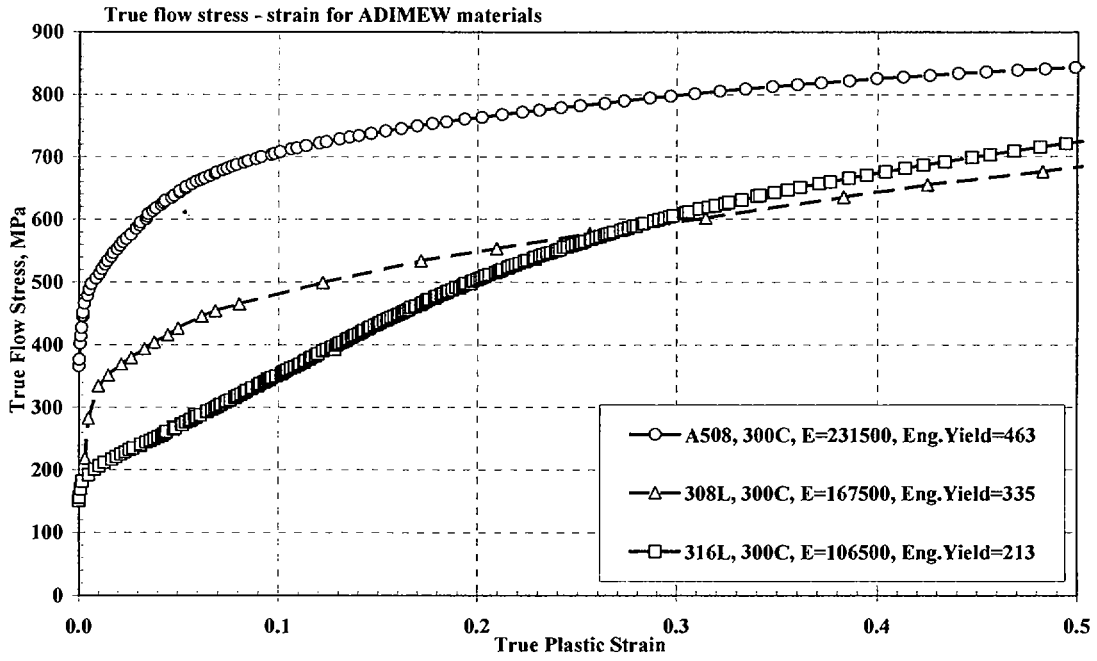

Figure 8: Tensile behaviour for the various constituents of the mock-up at 300°C test temperature

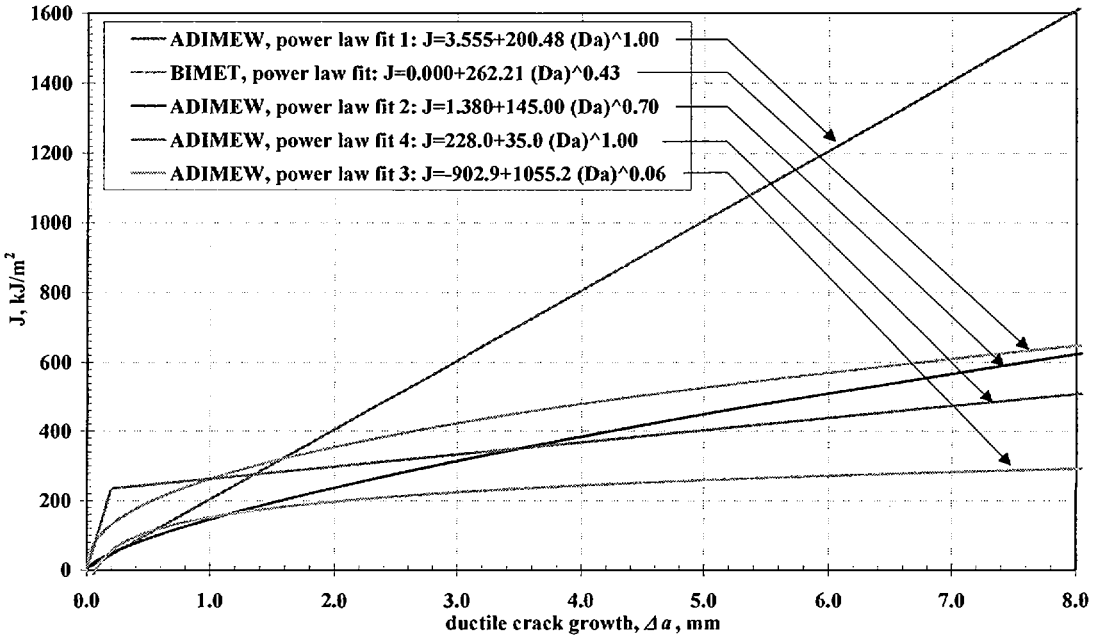

Figure 9: Five fracture toughness resistance curve fits for weld buttering used in assessments

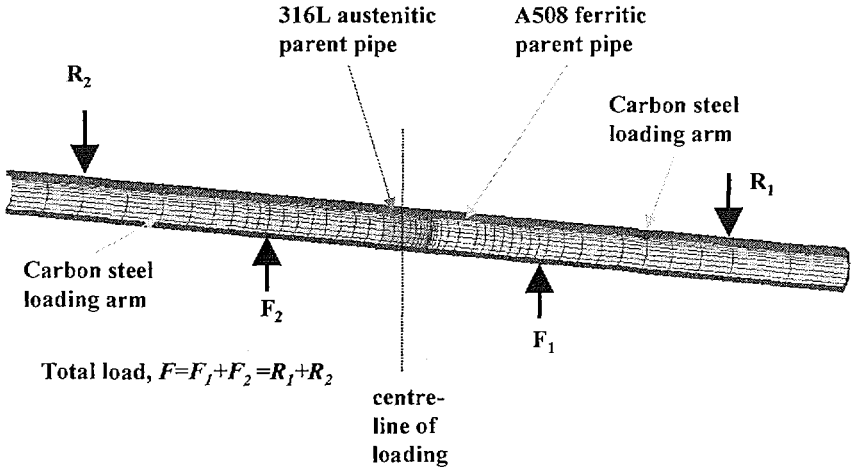

Figure 10: Overall finite element mesh used, showing loading and restraint positions

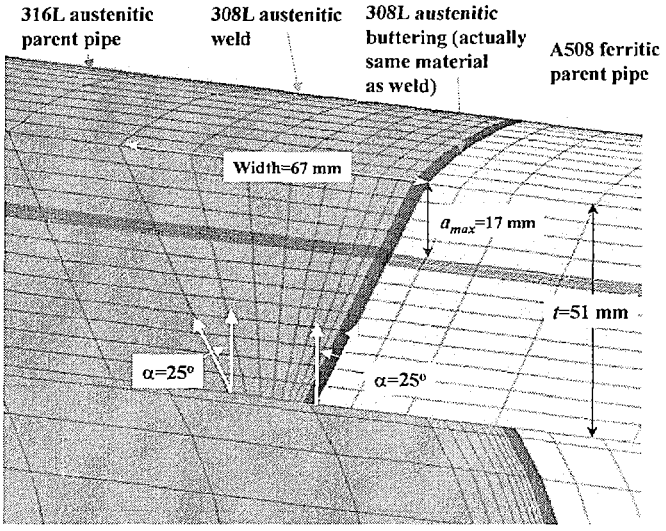

Figure 11: Close-up of mesh near initial 17 mm deep defect in dissimilar metal weld buttering

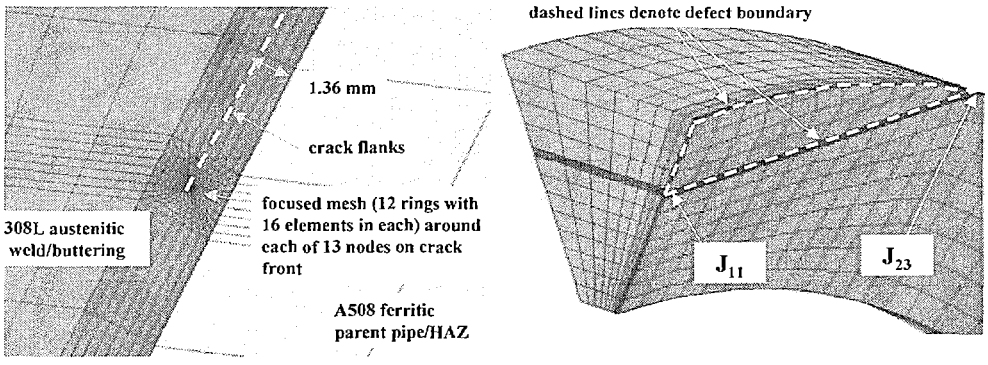

Figure 12: Left picture shows focused mesh around crack front. Right picture is section through plane of defect, showing weld metal only: with 13 nodes on (half) crack front from 'J11' at middle to 'J23' on outer pipe surface

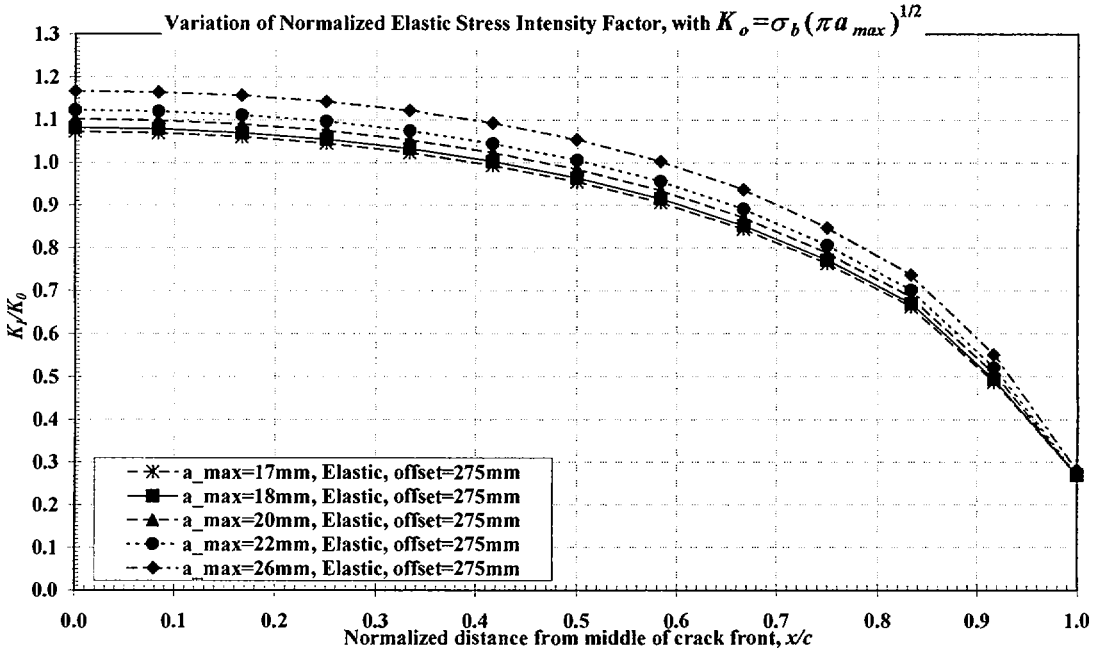

Figure 13: Variation of elastic stress intensity factor along crack front for different a_{max}

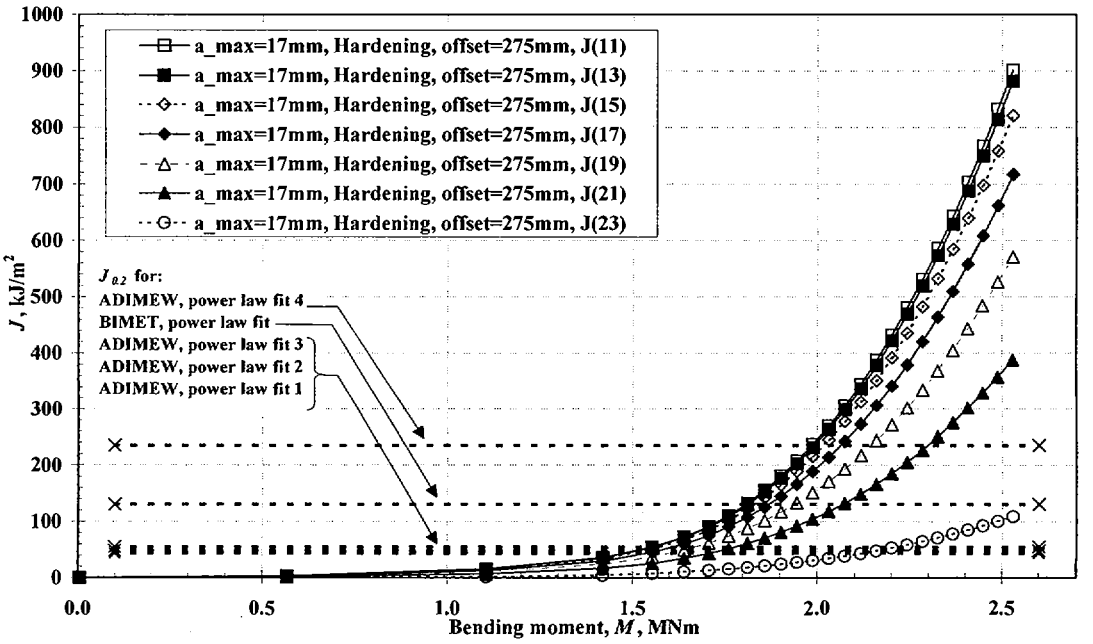

Figure 14: Variation of *J* with *M* at every 2nd crack front node for a_{max}=17 mm, showing initiation $J_{0.2}$ levels for the various *J*-R curve fits

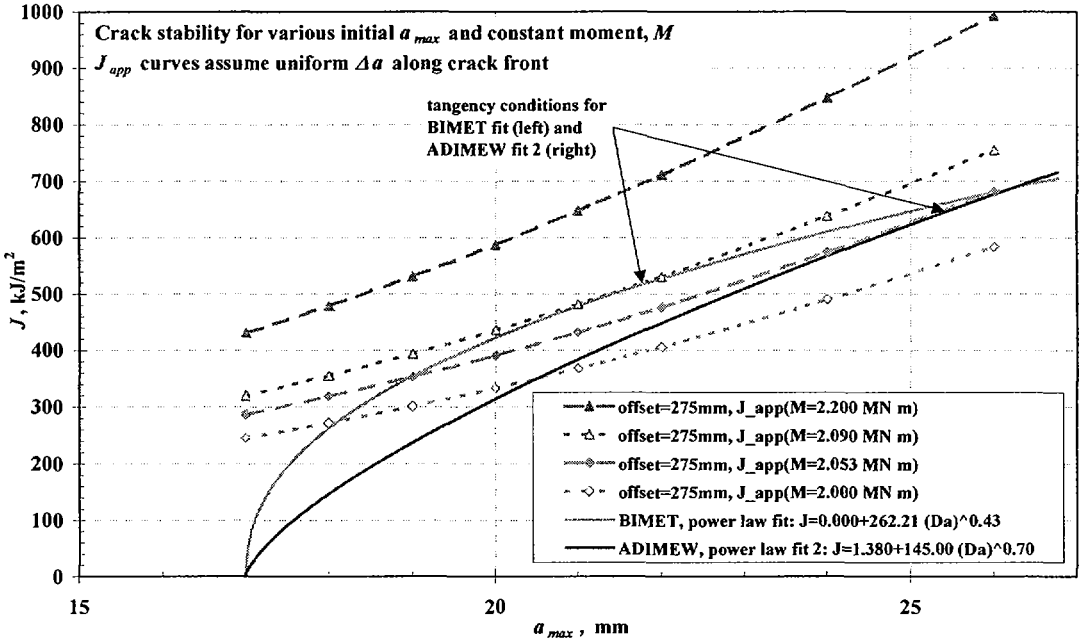

Figure 15: Comparison of two buttering *J*-R curve fits with applied *J* versus a_{max} for four constant values of moment, showing two tangency conditions

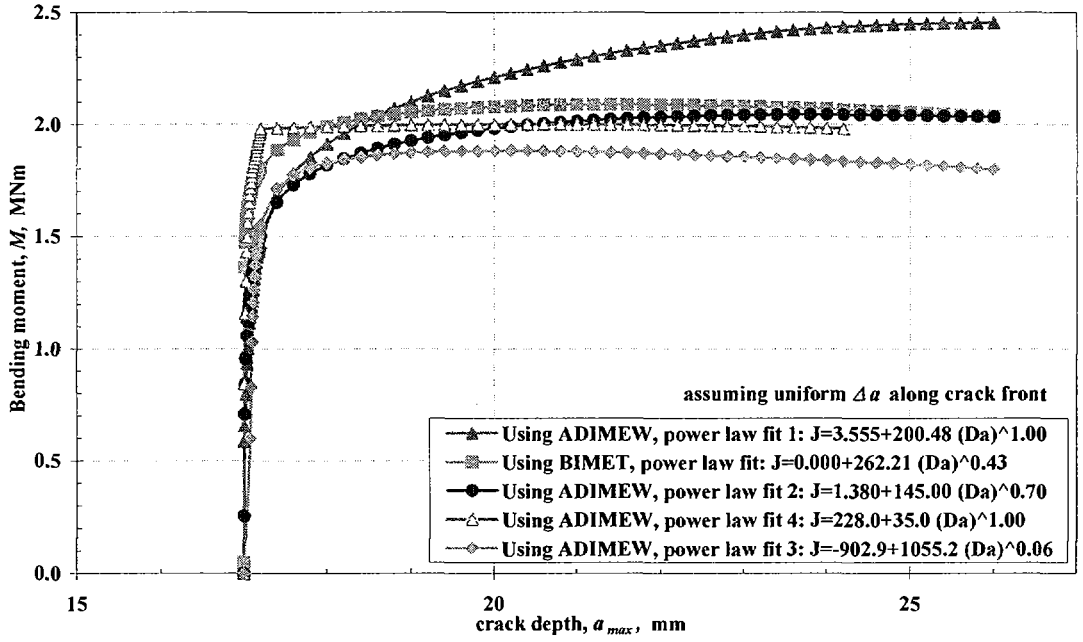

Figure 16: Bending moment versus crack depth predictions for the five buttering *J*-R curve fits considered

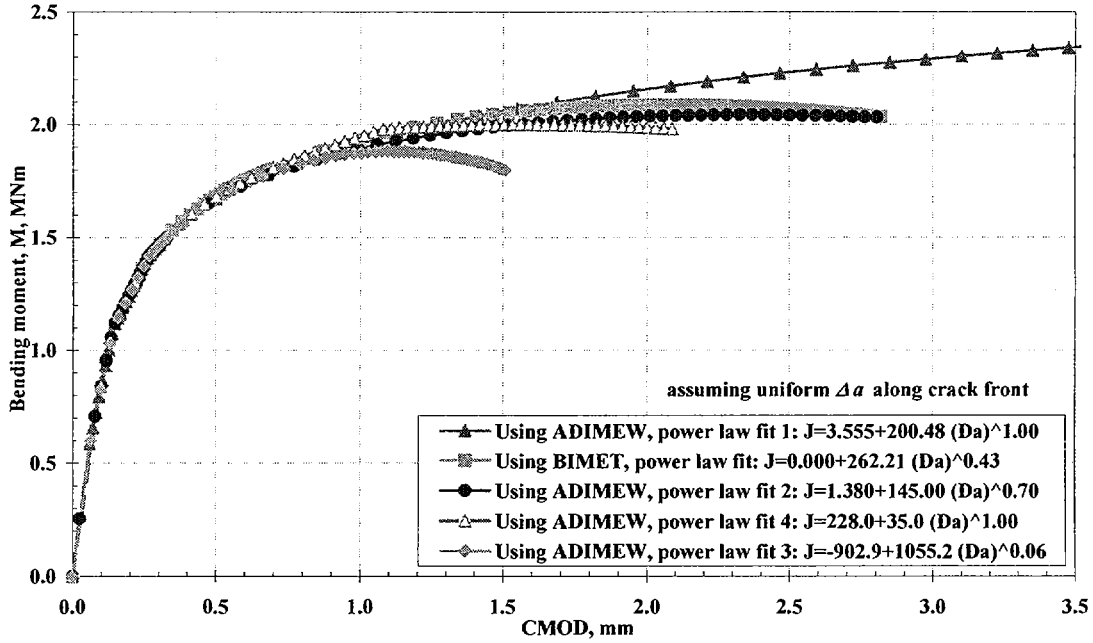

Figure 17: Bending moment versus crack mouth opening displacement predictions for five buttering *J*-R curve fits

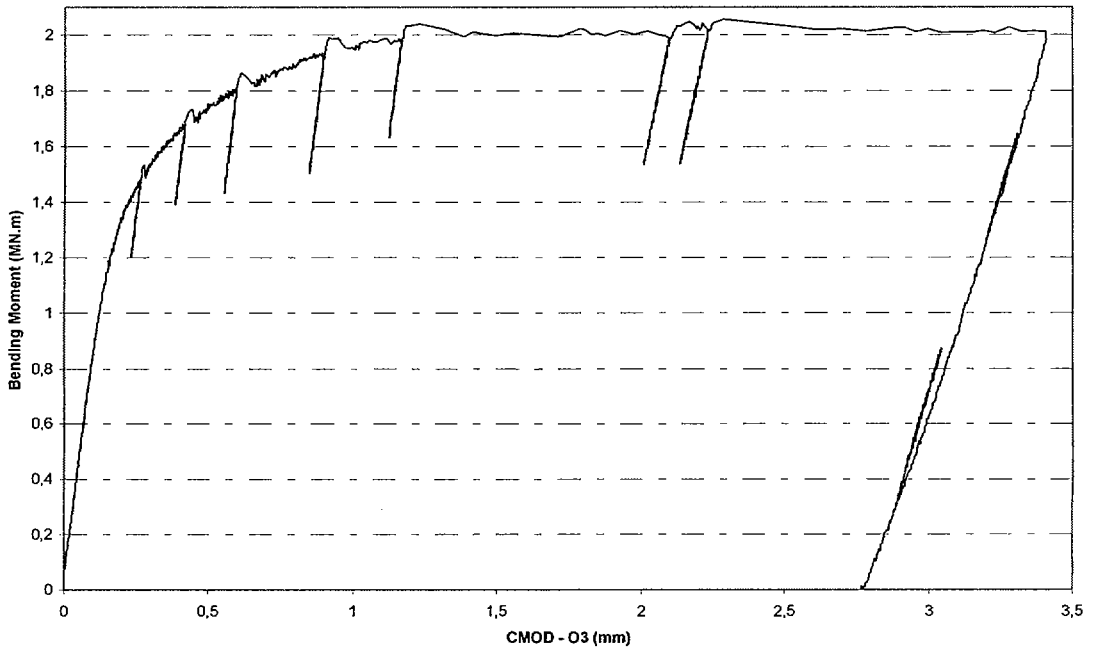

Figure 18: Bending moment versus EdF crack mouth opening displacement measurements from ADIMEW test

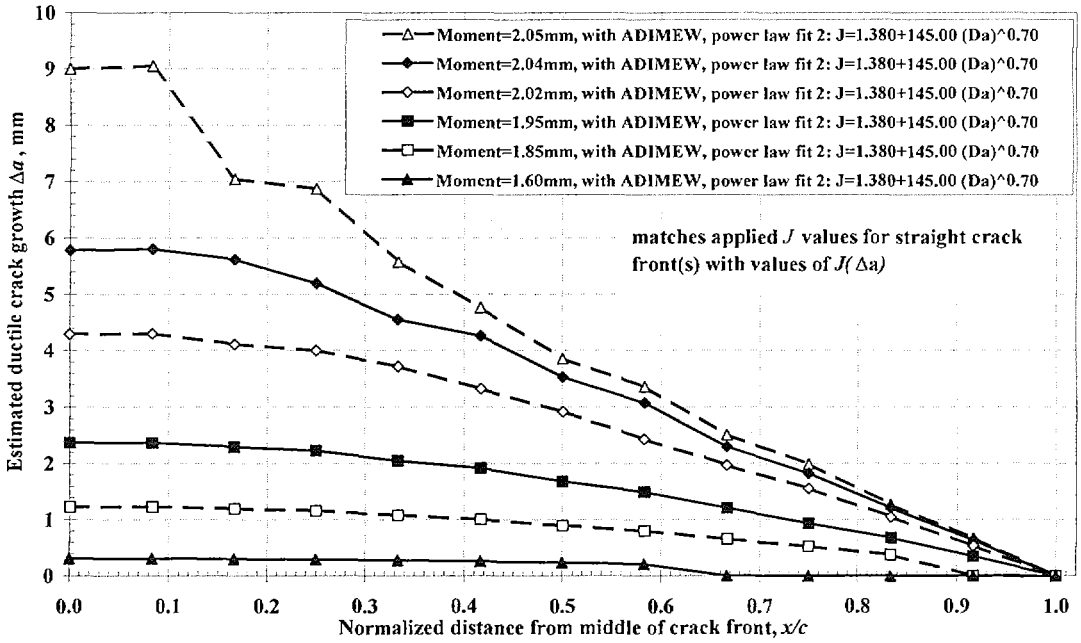

Figure 19: Estimated crack growth profiles using the finite element values for applied *J* and 'ADIMEW fit 2' weld buttering *J*-R curve; profiles are shown as a function of increasing bending moment

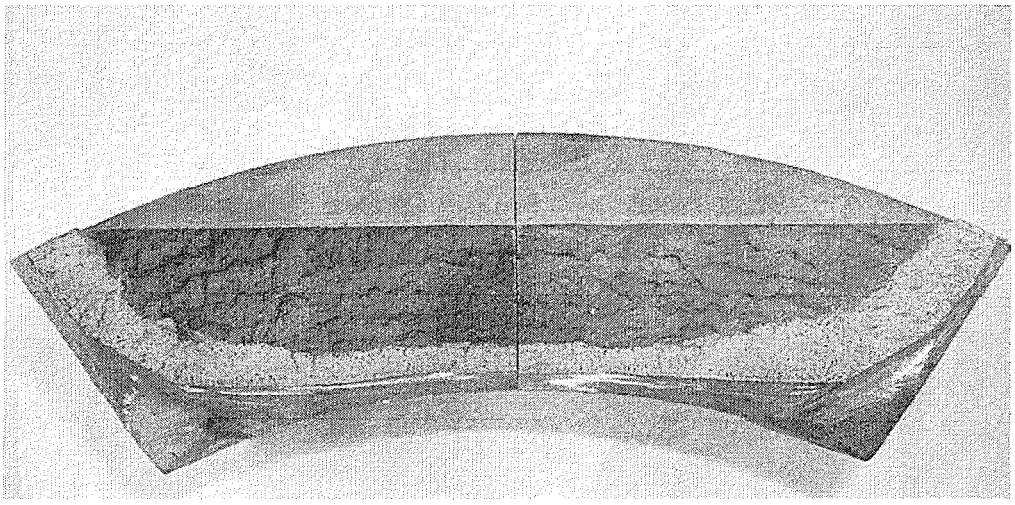

Figure 20: Post-test fracture face of the actual ADIMEW test pipe